Distribution Category:
Plasma Fusion Systems
UC-421
Magnetic Fusion Reactor Materials
UC-423

ANL/FPP/TM-255

ANL/FPP/TM--255

DE91 017235

ARGONNE NATIONAL LABORATORY
9700 South Cass Avenue
Argonne, Illinois 60439-4801

ITER DIVERTOR SPUTTERING EROSION - RECENT ANALYSIS FOR CARBON, BERYLLIUM, TUNGSTEN, AND NIOBIUM SURFACES

by

Jeffrey N. Brooks

Fusion Power Program
Engineering Physics Division

July 1991

Work supported by

Office of Fusion Energy
U.S. Department of Energy
Under Contract W-31-109-Eng-38

TABLE OF CONTENTS

LIST OF TABLES

LIST OF FIGURES

ITER DIVERTOR SPUTTERING EROSION - RECENT ANALYSIS FOR CARBON, BERYLLIUM, TUNGSTEN, AND NIOBIUM SURFACES

by

Jeffrey N. Brooks

ABSTRACT

ITER divertor plate sputtering erosion has been analyzed using current design information and updated impurity transport models. The REDEP[1,2] erosion/redeposition code was used to compute erosion for a very low plasma divertor temperature ($T_{e_c} \approx 12$ eV) physics phase "reference" case, and for other plasma conditions. A high surface temperature case ($T_{s_o} = 1800°$ C) is analyzed for a carbon surface. Niobium is analyzed using WBC[3] near-surface transport code results for the redeposited charge state. The REDEP results show high net erosion rates ($\gtrsim$ 20 cm/burn•yr) for beryllium and carbon, even at low plasma temperatures. Net erosion rates are low to moderate for niobium (~0-3 cm/burn•yr), depending on plasma conditions, and low for tungsten (~0 - 0.2 cm/burn•yr).

1. INTRODUCTION

A recent study[2] analyzed sputtering erosion for the proposed ITER device[4] in detail. That study examined effects of surface material, plasma conditions at the divertor, poloidal field sweeping, and other design issues. The work reported here represents a follow-on study to examine divertor erosion for the following conditions: 1) a somewhat modified divertor geometry (poloidal field angle $\alpha = 15°$ instead of 20°), 2) different divertor region plasma temperatures and, in particular, a very low temperature regime, 3) high surface temperature operation for carbon, and 4) a niobium surface. The new conditions have necessitated the development of additional models and computer code capability, in particular, the REDEP analysis now includes a more rigorous computation of the carbon erosion resulting from chemical sputtering and radiation enhanced sublimation. For the niobium analysis, it was necessary to develop estimates for redeposited ion charge states and energy - this was done via the WBC Monte Carlo code.[3]

In general, the present analysis shows qualitatively similar results as past studies with high erosion rates predicted for the low-Z materials and low rates for tungsten. Niobium always performs much better than carbon or beryllium and is similar to tungsten at the lower plasma temperature.

2. CARBON AND BERYLLIUM EROSION

Scrape off layer plasma transport code studies by Cohen et al.[5] and others e.g. Ref. (6), have identified the possibility of obtaining very low plasma temperatures at a high recycling, ITER type divertor. Peak electron temperatures at the divertor plate of $T_{e_o} < 15$ eV have been predicted. This is for "physics phase" operation with no supplemental plasma heating from current drive. The very low plasma temperature regime is characterized by a high density and high particle flux, necessary to convect roughly the same power to the divertor plate as the higher temperature cases. For low-Z materials, the higher particle flux offsets some of the advantage for erosion at low T_{e_o} arising from lower sputtering coefficients.

REDEP code erosion results for a carbon surface at $T_{e_o} = 12$ eV are shown in Fig. 1 for a peak surface temperature of $T_{s_o} = 1800°$ C. This case and others analyzed are summarized in Table 1. In this analysis the surface temperature is assured to scale linearly with heat flux. The peak surface

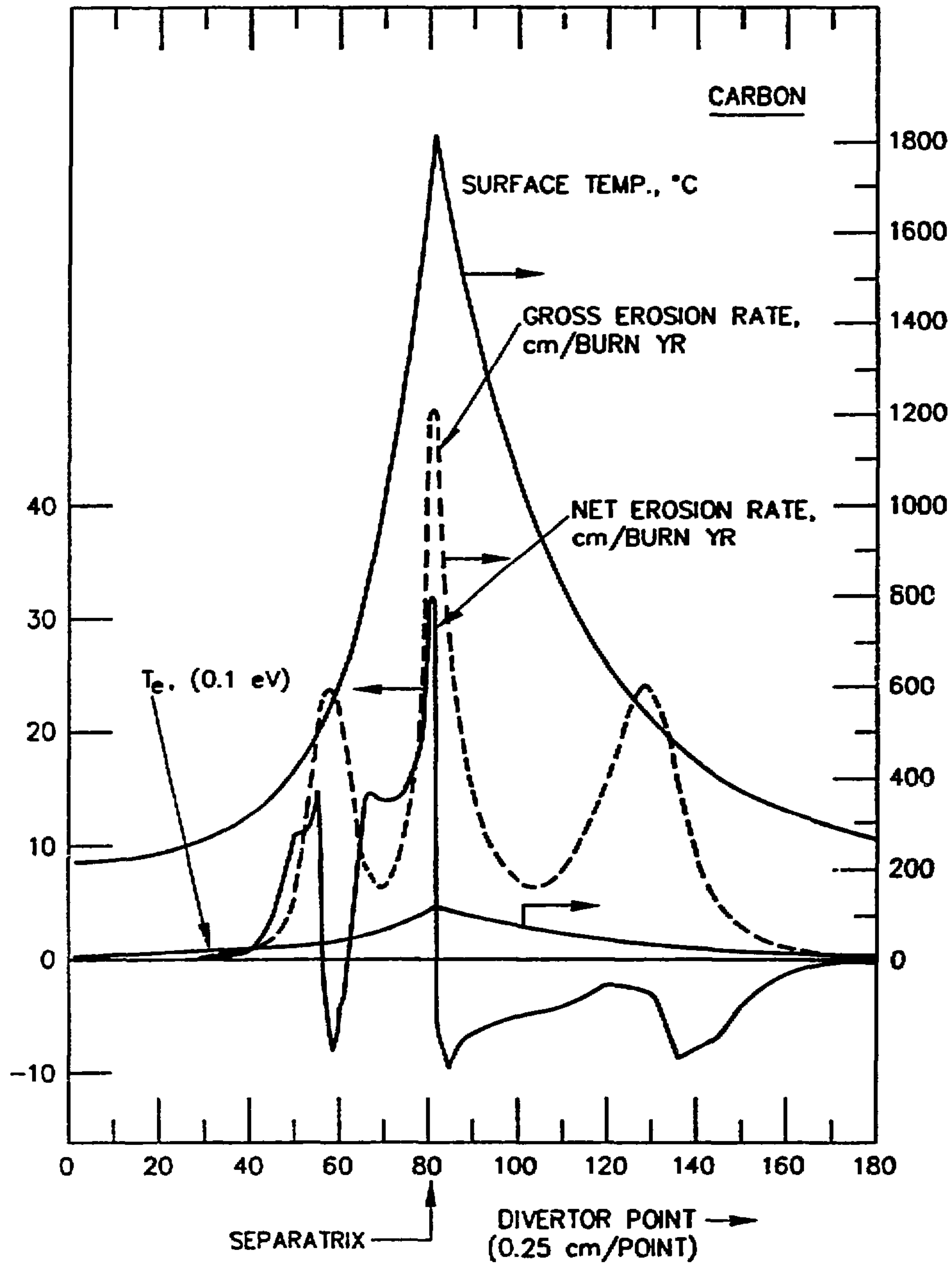

Figure 1. Erosion of a carbon coated divertor plate, for peak surface temperature, T_{s_o} = 1800°C, peak plasma electron temperature, T_{e_o} = 12 eV.

TABLE 1. ITER Divertor REDEP Analysis-Peak Erosion Rate Summary

Plate Material	Plasma Temp. (peak) T_{e_o}, eV	Plasma Density (peak) N_{e_o}, m^{-3}	Other Conditions*	Peak Gross Erosion Rate, cm/burn•year	Peak Net Erosion Rate, cm/burn•year	Comments
carbon	12	6×10^{20}	T_{s_o} = 1800° C**	1200	32	A, B
carbon	12	6×10^{20}	T_{s_o} = 1200° C	870	17	
beryllium	12	6×10^{20}		980	20	
niobium	12	6×10^{20}		5	<.02	
tungsten	12	6×10^{20}		2	<.02	C
carbon	25	3×10^{20}	T_{s_o} = 1800° C	2920	69	
carbon	25	3×10^{20}	T_{s_o} = 1200° C	890	29	
beryllium	25	3×10^{20}		982	31	
niobium	25	3×10^{20}		49	0.3	
tungsten	25	3×10^{20}		3	.03	
carbon	50	1.5×10^{20}	T_{s_o} = 1800° C	4020	208	
carbon	50	1.5×10^{20}	T_{s_o} = 1200° C	963	45	
beryllium	50	1.5×10^{20}		803	41	
niobium	50	1.5×10^{20}		135	2.5	D, E
tungsten	50	1.5×10^{20}		11	0.2	D, E
niobium	50	1.5×10^{20}	with sweeping ± 2 cm	83	1.1	
tungsten	50	1.5×10^{20}	with sweeping ± 2 cm	7	.08	

* All cases 0.1% oxygen, poloidal angle α=15°; 12 eV cases are ITER cases A1 & B1 (see Ref. 5) other cases scaled for constant peak heat flux, q_o=7.5 MW/m^2.

** Peak surface temperature.

Key to Comments

A - All carbon results include chemical sputtering and radiation enhanced sublimation where applicable.

B - All carbon results are highly uncertain due to redeposited material property uncertainties at the very high gross erosion rates shown.

C - Most tungsten sputtering in this regime is due to oxygen.

D - Results depend critically on oblique-field sheath/near surface transport models (e.g. Ref. 3).

E - All niobium and tungsten results show negligible sputtered impurity fluxes to core plasma.

temperature occurs at the strike point and is treated as an independent variable. Both physical sputtering, chemical sputtering, and radiation enhanced sublimation (RES) are included in the calculation.

The redeposition of chemically sputtered carbon and RES carbon is computed in REDEP by solving transport equations for thermally sputtered methane neutrals and carbon neutrals respectively. In the case of methane, ionization by electron impact and hydrogen-methane charge exchange is treated. The calculation represents an advance over previous work which simply assumed 100% local redeposition. Additional work is needed however, to eventually include the effects of the full set of relevant hydrocarbon atomic processes.

As shown in Fig. 1, the gross erosion rate for carbon has three peaks. The central peak is due to physical sputtering plus RES and the side peaks are due primarily to chemical sputtering. The gross erosion rate is very high and this raises questions concerning the stability and characteristics of the redeposited surface. As with previous REDEP analysis, the net erosion rate calculation assumes that the redeposited surface has identical sputtering properites to the original graphite and is mechanically stable. As discussed in References 2 and 7, this is a reasonable assumption at present, but experimental work is necessary to study this issue.

Since the peak divertor surface temperature depends, in part, on coating thickness, there is a potential tradeoff between erosion lifetime and surface temperature. As shown in Table 1, however, a peak surface temperature of 1200° C (achieved with a thinner initial coating thickness) reduces the net erosion by about a factor of two compared with results for T_{s_o} = 1800° C. This is due primarily to the elimination of RES at the lower surface temperature. Results (not shown) for a surface temperature of T_{s_o} = 800° C are similar to T_{s_o} = 1200° C. The increased erosion rate at higher surface temperatures obviously negates some or all of the lifetime advantages of a thicker coating, for carbon.

Erosion analysis was performed for two higher plasma temperatures, as summarized in Table 1. (These cases assume a somewhat different density scaling with plasma temperature then Ref. (2).) Higher plasma temperatures result in substantially higher erosion rates, due primarily to an increase in sputtering coefficients and secondarily to a decrease in redeposition at lower electron densities.

A beryllium divertor surface was analyzed for the same range of plasma conditions as carbon. No surface temperature dependent effects are included i.e. all sputtering is physical sputtering. As shown in Table 1, erosion rates for beryllium are of the same magnitude as carbon.

3. NIOBIUM AND TUNGSTEN EROSION

In support of the REDEP analysis of a niobium divertor surface, the WBC code was used to compute redeposited charge states, incident angles, and incident energy for sputtered niobium particles. This code completes the sub-gyro orbit motion of impurity atoms and ions in a fixed D-T plasma background, with oblique magnetic field and sheath electric field. Impurity ion-plasma collisions are treated in detail as well as relevant atomic processes.

Typical WBC code results for niobium are shown in Table 2. The near-surface sputtered niobium transport appears to be very similar to tungsten. In particular, sputtered particle ionization occurs primarily within the magnetic sheath, redeposited charge states are low, and self-sputtering coefficients are less than unity, for the plasma conditions examined. These results were used for the REDEP analysis of niobium.

REDEP results for niobium and tungsten divertor surfaces are shown in Fig. 2 for T_{e_o} = 50 eV, and are summarized in Table 1 for all cases. The substantial differences between niobium and tungsten performance at T_{e_o} = 50 eV is due to the ~10 x higher D-T sputtering coefficients for niobium. Thus, although self-sputtering appears to be reasonable for niobium at T_{e_o} = 50 eV (i.e. no runaway condition) net erosion rates are ~10 x higher than for tungsten. This ratio also holds at T_{e_o} = 25 eV, however the net erosion rate for niobium decreases by a factor of ~10 due to the steep fall of light particle sputtering coefficients in the plasma temperature regime. Finally, for T_{e_o} = 12 eV the net erosion rates for tungsten and niobium are similar and are both very low, being due mostly to oxygen (or similar Z material) sputtering.

An advantage of niobium and tungsten over beryllium and carbon, in addition to lower peak erosion, is that their erosion profile is narrower (due to steeper sputtering coefficient falloff with energy, along the divertor plate). As a result poloidal field sweeping to reduce erosion can be relatively more effective for the high Z materials. Table 1 summarizes the

Table 2. Redeposited Ion Parameters for Niobium, from WBC Code Analysis. For Plasma Parameters $N_{e_o} = 10^{20}\ m^{-3}$, $\psi = 87°$, $f_D = 0.25$, $e\phi_o = -3\ kT_e$; See Ref. 3 for Parameter Definition.

Parameter*		Value $T_e = 25$ eV	$T_e = 75$ eV
Neutral ionization distance (perpendicular to surface)	$\bar{z}_o$	.38 mm	.44 mm
Transit time	$\bar{\tau}_R$	.76 μs	.49 μs
	$\tau_{R_{SD}}$	1.3 μs	1.2 μs
Elev. angle	$\bar{\theta}$	26°	19°
Charge state	$\bar{K}$	2.3	2.3
	K_{SD}	1.5	2.3
Energy	$\bar{U}$	217 eV	507 eV
	U_{SD}	210 eV	664 eV
Self-Sputtering Coeff.	$\bar{Y}_{Nb \to Nb}$	.33	.73

* Bar denotes average value, SD denotes standard deviation.

results for a modest sweep parameter, for niobium and tungsten. As shown, a factor of 2-3 reduction in erosion is obtained for a ± 2 cm sweep distance. Longer sweep distances would be expected to further reduce the time-averaged peak erosion rates.

4. DISCUSSION

As discussed in Ref. 1, 2 there is less concern about the integrity of a redeposited beryllium surface than for carbon. Potentially high self-sputtering coefficients at oblique incident angles are a concern, however, for beryllium.

The present REDEP analysis for beryllium incorporates self-sputtering coefficients computed by the DSPUT code.[8] A recent analysis of beryllium self-sputtering[9] using a coupled rough surface code (fractal-TRIM) and near-surface plasma transport code (WBC) predicts higher values of self-sputtering than DSPUT. There is insufficient experimental data on oblique-incidence beryllium self-sputtering to validate either model. The WBC/F-TRIM results would imply worse beryllium erosion than shown.

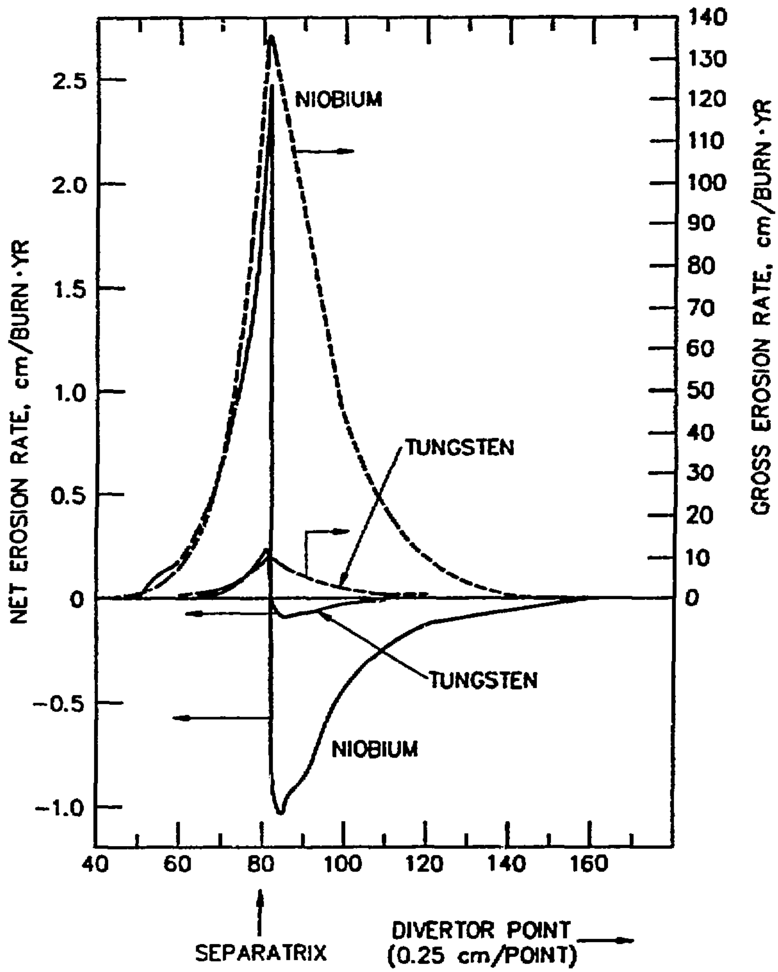

Figure 2. Erosion of niobium and tungsten divertor plate surfaces, for T_{e_0} = 50 eV.

5. CONCLUSION

This study has updated an earlier analysis of ITER divertor sputtering erosion for recently defined design conditions and, in the case of niobium, for a different candidate material. As with previous studies, the analysis has several key uncertainties associated with plasma boundary and material behavior (see Ref. 2), but should be reliable enough to identify basic trends.

A very low plasma divertor temperature is indeed found to be helpful for reducing low Z material sputtering. Sputtering erosion rates for beryllium and carbon are high enough, however, to necessitate either frequent divertor plate changeouts, and/or in-situ recoating. High surface temperature operation of carbon, resulting from a thicker carbon coating, causes a substantial increase in erosion rates and is therefore possibly counter-productive. In general, the use of carbon and beryllium would appear to be limited to ITER physics phase (low availability) operation only.

A tungsten divertor surface continues to appear desirable, from the standpoint of sputtering erosion. Tungsten combines finite self-sputtering, for the plasma regime studied, with low light ion sputtering. Modest sweep rates further reduce tungsten erosion. A tungsten surface would function well over the plasma divertor temperature regime examined, T_{e_o} = 12-50 eV, according to this study.

Niobium erosion is much lower than carbon or beryllium, due to lower light ion sputtering coefficients. Niobium performance is similar to tungsten at T_{e_o} = 12 eV where erosion of both materials is due primarily to a trace oxygen content. Niobium erosion is ten times higher than tungsten at T_{e_o} = 25 eV but may still be acceptably low, for example a 3 mm thick niobium surface would last ~1 burn•yr without sweeping, and about 3 burn•yr with only modest (± 2 cm) sweeping. Niobium performance appears marginal at T_{e_o} = 50 eV.

6. REFERENCES

1. J.N. Brooks, Nucl. Tech./Fusion 4 (1983) 33.
2. J.N. Brooks, Fus. Tech. 18 (1990) 239.
3. J.N. Brooks, Phys. Fluids B 2 (1990) 1858.
4. J.R. Gilleland et al., Nucl. Fusion 29 (1989) 1191.

5. S. Cohen, K.A. Werley, D.E. Post, B.J. Braams, J.L. Perkins, and D. Pearlstein, J. Nuc. Mat. 176&177 (1990) 909.

6. M.F.A. Harrison and E.S. Hotson, ibid, P256.

7. J.N. Brooks, H.F. Dylla, A. Pontau, and K. Wilson, Fus. Tech. 19 (1991) 1095.

8. D.L. Smith, J.N. Brooks, D.E. Post, and D.B. Heifetz, Proc. 9th Symposium on Engineering Problems of Fusion Research, IEEE Pub. No. 81CH1715-2 (IEEE New York, 1981) P719.

9. J.N. Brooks and D.N. Ruzic, J. Nucl. Mat. 176&177 (1990) 278.

DISTRIBUTION LIST FOR ANL/FPP/TM-255

Internal

H. Attaya
M. Billone
J. Brooks (10)
H. Chiu
D. Ehst
P. Finn
Y. Gohar
D. Gruen
A. Hassanein
T. Hua
A. Hull
C. Johnson
A. Krauss
L. LeSage
B. Loomis
S. Majumdar
R. Mattas
B. Picologlou
C. Reed
D. Smith
D. Sze
L. Turner
FPP Files (15)
ANL Contract File
ANL Patent Dept.
TIS Files (3)

External

DOE-OSTI, for distribution per UC-421 and UC-423 (50)
Manager, Chicago Operation Office
ANL-TIS Libraries
C. Baker, Oak Ridge National Laboratory
R. Causey, Sandia National Laboratories, Livermore
M. Cohen, Office of Fusion Energy, DOE
S. Cohen, Princeton Plasma Physics Laboratory
K. Dimmof, Institute National de la Recherche Scientifique
A. Haasz, University of Toronto
M. Harrison, Culham Laboratory
Y. Hirooka, University of California, Los Angeles
W. Hsu, Sandia National Laboratories, Livermore
D. Manos, Princeton Plasma Physics Laboratory
R. McGrath, Sandia National Laboratories, Albuquerque
R. Nygren, Sandia National Laboratories, Albuquerque
K. Parbhakar, Institut National de la Recherche Scientifique
P. Stangeby, University of Toronto
M. Ulrickson, Princeton Plasma Physics Laboratory
K. Wilson, Sandia National Laboratories, Livermore
J. Winter, c/o General Atomic
C. Wong, TSI Research
Bibliothek, Max-Planck-Institute fur Plasmaphysik, Germany
Bibliothek, Institute fur Plasmaphysik, KFA Julich, Germany
C.E.A. Library, Fontenay-aux-Roses, France
Librarian, Culham Laboratory, England
Library, Commission of the European Community, Italy
Thermonuclear Library, Japan Atomic Energy Research Institute, Japan